

# Propene Polymerization with Silica-Supported Metallocene/MAO Catalysts

Gerhard Fink,\* Bernd Steinmetz, Joachim Zechlin, Christian Przybyla, and Bernd Tesche

Max Planck Institut für Kohlenforschung, Kaiser-Wilhelm-Platz 1, D-45470 Mülheim/Ruhr, Germany

Received September 9, 1999

## Contents

I. Introduction	1377
II. Silica Gel as Supporting Material	1379
A. Physical and Chemical Properties	1379
B. Particle Form, Surface and Bulk Structure	1380
III. Supporting Methods and Procedures	1381
A. Suspension Impregnation	1382
B. Gas-Phase Impregnation	1383
IV. Polymerization Kinetics	1383
V. Polymer Morphology	1384
VI. Fragmentation Process	1387
VII. Conclusions	1388
VIII. Acknowledgment	1390
IX. References	1390

## I. Introduction

The production of polyolefins such as polyethylene (PE) or polypropylene (PP) and their copolymers increases continuously due to their outstanding product properties and their environmental compatibility. They are commonly applied as packing material, foils, fibers, as well as components for the automotive and electrical industry. In 1996 the worldwide production of PE and PP counted 40 million and 20 million tons, respectively. On the basis of the global demand,<sup>1</sup> the growth rate of PP production is predicted to rise up to 7% per year until 2002/2003.

Polyolefins are commercially produced either by employing the classical heterogeneous Ziegler catalysts on MgCl<sub>2</sub> support or by using chromium catalysts on SiO<sub>2</sub> or Al<sub>2</sub>O<sub>3</sub> supports, which are better known as Phillips catalysts. With the introduction of Achieve, a metallocene-catalyzed polypropylene (mPP), in 1995 Exxon Chemical has taken the first step toward a new catalyst generation.<sup>2</sup> Only two years later Targor GmbH was the first company in Europe to make metallocene polypropylene commercially available.<sup>3</sup> The success of metallocene mainly depends on the fact that the modern PP technologies and plants of gas-phase and slurry reactors can be used for heterogeneous metallocene catalysts (so-called drop-in catalysts).<sup>4,5</sup> This will certainly speed up the replacement of the PP pro-

duced by Zieglercatalysts. According to the neutral estimations, in 10 years 20% of the standard PP will be synthesized applying supporting metallocene catalysts.

The major objective of the heterogenization process was, on the one hand, to preserve the advantages of homogeneous metallocenes, such as the high versatility and flexibility of the corresponding synthesis, the ability to control polymer microstructure, and their high activity. On the other hand, it was intended to combine these features with the properties of supported catalyst technologies (good morphology, little reactor fouling, high powder density).

Amorphous and porous SiO<sub>2</sub> at present constitute the best support for metallocenes and MAO as cocatalyst because they possess a high surface area and porosity, have good mechanical properties, and are stable and inert under reaction and processing conditions.<sup>6–8</sup> As a result of immobilization, the metallocene/MAO molar ratio can be decreased by approximately 2 orders of magnitude as compared to homogeneous systems.<sup>9,10</sup> In certain cases, 40 equiv is already sufficient to obtain reasonable polymer activities. Nevertheless, less common supporting materials were analyzed along with the classical MgCl<sub>2</sub> and Al<sub>2</sub>O<sub>3</sub> materials.<sup>11</sup> Examples are zeolites<sup>12–14</sup> and polymeric aluminoxanes.<sup>15</sup> Attempts were also carried out to imitate the surface of silica by using cyclodextrine<sup>16</sup> and polysiloxane derivatives.<sup>17</sup> Most recent experiments employ cross-linked polystyrene as supporting material for metallocene catalysts.<sup>18,19</sup> A new method for the preparation of heterogeneous catalysts is the approach of self-immobilizing metallocene catalysts. The metallocenes containing alkenyl substituents are incorporated as comonomers into the formed polyolefin chain.<sup>20–22</sup> Many of these supports yielded agreeable polymer morphologies but lacked activities similar to the ones of the SiO<sub>2</sub> support.

Heterogenization has increased the complexity of metallocene-catalyzed systems, as it has added the influence of the support and the supporting method (Figure 1). This review will summarize how and by which parameters polymerization kinetics, polymer growth, polymer morphology, and particle fragmentation are influenced. This article focuses on the research performed in our group, since we believe that we have contributed to a great extent to the



Gerhard Fink, born 1939, obtained his Doctor in Chemistry degree (Dr. rer. nat.) from the Technical University of München in 1969 with a biophysical thesis under the direction of Franz Patat. In 1977 he became recognized as an academic lecturer (Habilitation) for Chemistry from the same University with work on Elementary steps in Ziegler–Natta catalysis. Since 1980 he has been the head of the Macromolecular research group at the Max-Planck-Institut für Kohlenforschung in Mülheim a.d. Ruhr, Germany. He is apl. Professor at the University of Düsseldorf and lectures for Macromolecular Chemistry. His areas of reasearch include the following: Kinetics, mechanisms, elementary processes; Homogeneous and heterogeneous polymerization catalysis inclusive reaction modeling; Sterospecific polymerization; and Reaction engineering



Bernd Steinmetz was born in Saarbürg, Germany, in 1969. He studied Chemistry at the Heinrich- Heine University of Düsseldorf and University of California at Davis and received his Diploma in 1996. He earned his Ph.D. degree in polymer chemistry in 1999 working with Professor Gerhard Fink at the Max-Planck-Institut für Kohlenforschung in Mülheim. His doctoral thesis concerned the investigation of polypropylene growth of SiO<sub>2</sub>-supported metallocene catalysts by means of electron microscopy.



Joachim Zechlin was born in Essen, Germany, in 1970. He finished his Ph.D. work in 1999 at the Max-Planck-Institut für Kohlenforschung in Mülheim a.d. Ruhr under the direction of Professor Gerhard Fink. His work was focused on kinetic investigations of propylene polymerization with silica-supported metallocene catalysts. Since 1999 he has been working for the Bayer AG in Dormagen, Germany.



Christian Przybyla was born in Duisburg in 1969. He obtained his Ph.D degree in chemistry in 1998 under the direction of Professor Gerhard Fink (1999) at the Max-Planck-Institut für Kohlenforschung in Mülheim a.d. Ruhr, with his thesis work on the kinetics and polymer growth on silica-supported metallocene catalysts. Since 1999 he has been working at a forensic science institute.



Bernd Tesche was born in Haan, Germany, in 1943. In 1967 he received his degree in physical engineering from Staatliche Ingenieur Schule Lübeck. In 1981 he received his Dr. rer. nat. degree from Freie Universität Berlin under Professor H. G. Wittmann. From 1967 to 1970 and 1971 to 1975 he was a Scientist at the Fritz-Haber-Institut der Max-Planck-Gesellschaft, Berlin, Department of Electron Microscopy (Professor Dr. E. Ruska). From 1970 to 1971 he was a Group Leader at Edelstahlwerke Witten A. G., Witten, Department of Electron Microscopy (Dr. L. Rademacher). From 1975 to 1994 he was a Scientist and Group Leader at the Department of Electron Microscopy (Prof. Dr. E. Zeitler). From 1994 to present he has been a Scientist and Group leader at the Max-Planck-Institut für Kohlenforschung, Mülheim/Ruhr, Department of Electron Microscopy (Professor Dr. M. T. Reetz). His fields of research include the following: Characterization of catalytic materials using electron microscopy (HRTEM, SEM) as well as SPM (STM/AFM) and computer image analysis; Development of specimen preparation procedures for obtaining three-dimensional structure information by pattern recognition and computerised tomography.; and Application of these techniques for the investigation of catalytic reactions.

understanding of the polymerization behavior of SiO<sub>2</sub>-supported metallocene catalysts. The conditions chosen for the slurry polymerization of propene (low temperature, low catalyst concentration, low monomer concentration) facilitated a time-resolved representation of the polymerization and its various stages. It is only after detailed electron-microscopic and kinetic studies that the polymerization process could be interpreted and led to the development of a model for propene polymerization. Most references have been taken from the literature from 1991 onward.

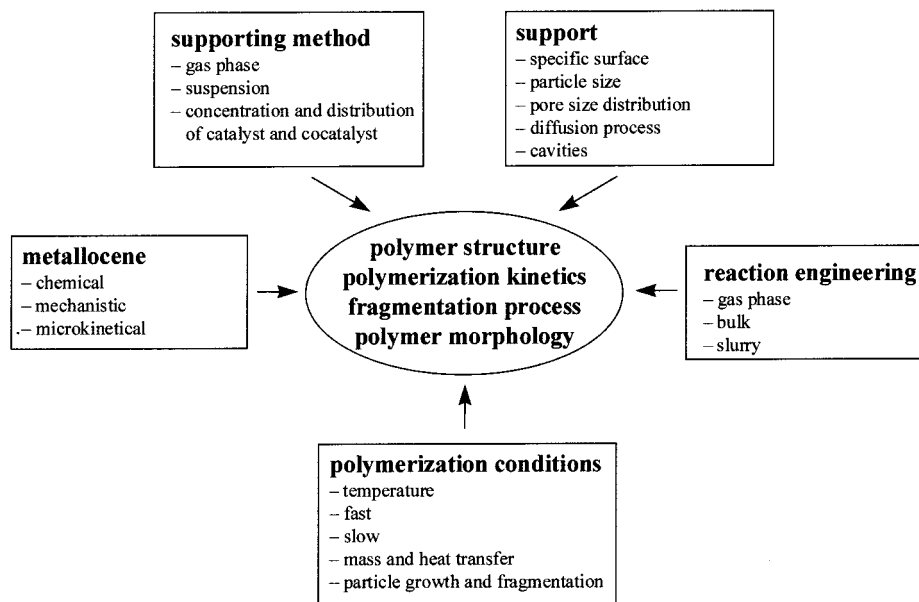


**Figure 1.** Parameters which influence polymerization kinetics, polymer structure, polymer morphology, and the fragmentation process of a silica-supported metallocene/MAO catalyst during olefin polymerization.

## II. Silica Gel as Supporting Material

### A. Physical and Chemical Properties

The right choice of supporting material as well as the choice of suitable properties (pore size, specific surface, chemical surface composition) are important factors influencing the immobilization of the metallocene catalyst and the fragmentation of the support during polymerization. Commercially applied porous silica gels are prepared by neutralization of aqueous alkali metal silicate with acid. The pore structure and pore size distribution can be controlled by the type of chemical reaction and experimental conditions.<sup>23,24</sup>

The pore size distribution is very narrow: it ranges from 1 to 20 nm.<sup>25</sup> The pores can therefore be classified as micro- and mesopores.<sup>26</sup> These pores are substantially responsible for the high specific surface which ranges from 250 to 1000 m<sup>2</sup>/g, depending on whether micro- or mesopores prevail. The chemical properties of amorphous silica are mostly governed by the chemistry of its surface, especially by the presence of silanol groups. A change in structure due to thermal or subsequent chemical treatment can strongly alter the properties. Therefore, it is possible to broaden the field of application for metallocene-supporting materials. The composition of silanol groups on the inner and outer surface of the silica gels was analyzed by paramagnetic samples,<sup>27,28</sup> infrared spectroscopy,<sup>29,30</sup> and titration.<sup>27,6</sup> Figure 2 shows the thermally induced change of a silica gel surface from silanol to siloxane.

The surface of pure silica gel is covered with silanol groups, at a maximum concentration of 8 Brønsted acid OH groups per nm<sup>2</sup>.<sup>31</sup> They are mostly found as geminal or isolated pairs and are neither very acidic nor very basic ( $pK_a \approx 6$ ). The hydroxylated surface is hydrophilic and easily adsorbs moisture from the air. This physically adsorbed water can be desorbed by raising the temperature to 100–200 °C. In the course of this heating a partial dehydroxylation of

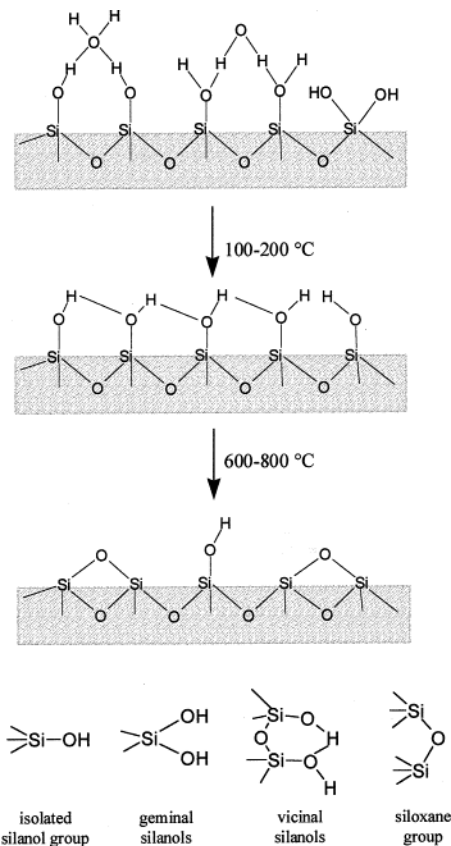


**Figure 2.** Schematic representation of the dehydration of a silica gel surface.

the silica gel takes place, reducing the number of OH groups per nm<sup>2</sup> to approximately 5.5 (approximately 5 wt % silanol groups attached to 300 m<sup>2</sup>/g silica). One-half of these OH groups are geminal pairs; the other half are vicinal ones. The number of hydroxyl groups decreases continuously as the temperature is raised, until at a temperature of 600–800 °C an almost completely dehydroxylated silica with approximately 1 OH group per nm<sup>2</sup> is left. From this



silanol concentration onward the surface is hydrophobic.

## B. Particle Form, Surface and Bulk Structure

Porous silica gels used as supporting material for metallocene catalysts are applied in two particle modifications with different diameters: they are either irregularly formed granulates or spherical particles.

The edged granulates result from grinding the filter cake which is obtained during the drying process of the silica gel production. It is possible to extract the desired particle size using conventional methods such as air separation or sieving processes (Figure 3a). However, to obtain higher powder densi-

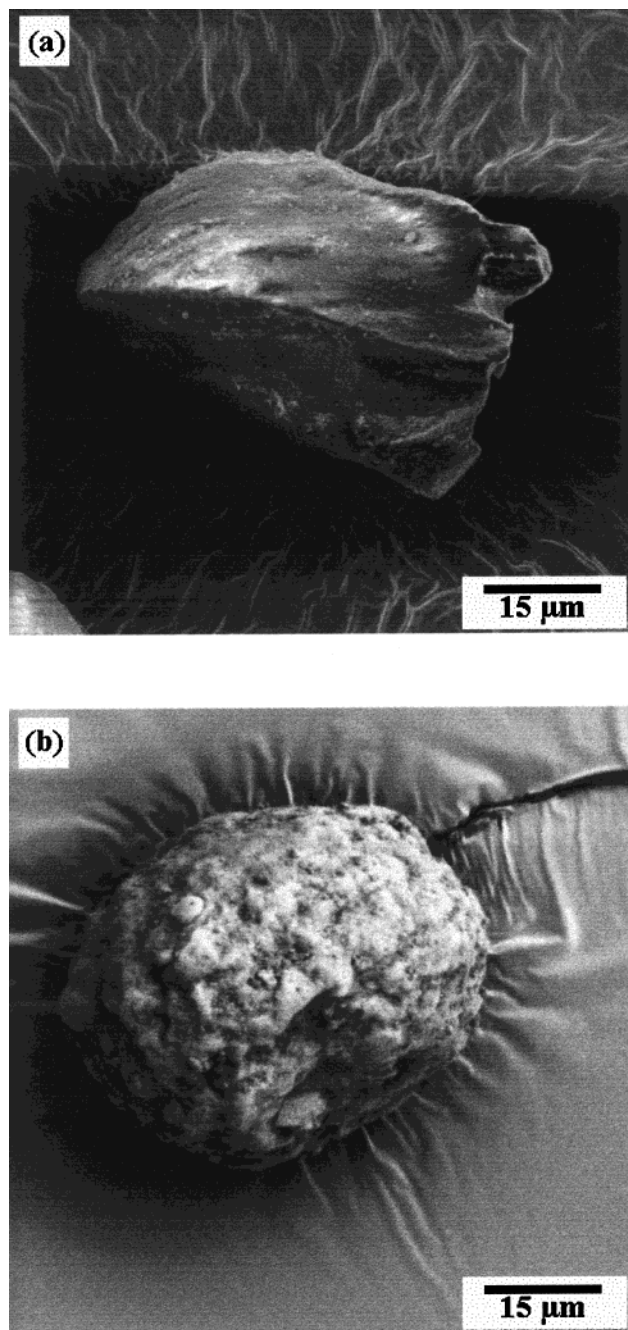


**Figure 3.** Morphological SEM micrographs of the (a) granular and (b) spray-dried silica gel.

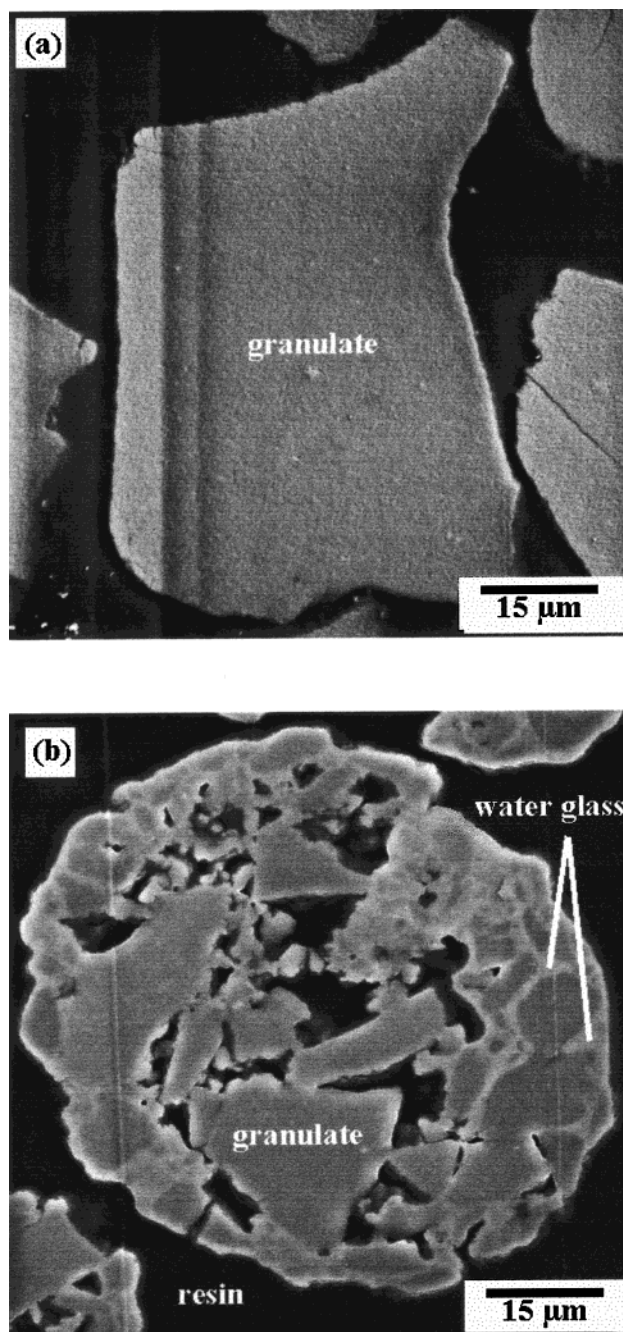


**Figure 4.** SEM micrographs of the bulk structure of the (a) granular and (b) spray-dried silica gel. The water glass serves as cement for the granulate fragments to form a spherical particle during the spray-drying process.

ties of these materials they are predominantly employed as spherical particles (Figure 3b). The granules are obtained by applying a spray-drying method or by emulsification of a silica sol in an immiscible nonpolar liquid.

In the course of the first method, the ground granulate particles of desired particle sizes ranging from 10 to 100  $\mu\text{m}$  are redispersed in a mineral acid and are subsequently dried using a spray-drying procedure.<sup>32</sup> For spray drying the wet stock is sprayed through a nozzle into a countercurrent of dry gas. This procedure yields a fine powder in a very short time. Particles can be prepared in the desired sizes of 10–100  $\mu\text{m}$ .<sup>33,34</sup> The second method of pelletizing starts with the emulsification of a silica sol in an

immiscible nonpolar liquid by stirring, dropping, etc., and converting the droplets being formed in this way into gelled beads of silica hydrogel. The particle size is controlled by the drop size and the viscosity of the sol.

Figure 4 shows the bulk structures of differently shaped silica gels. Considering the compact uniform volume structure, the granulated material clearly differs from the spherical silica. The spray-dried silica gels have a distinctive secondary bulk structure which derives from the cementation of larger granulate fragments. The size and shape of the resulting cavity structure depends on the size and size distribution of the employed granulates. Singular granulate fragments can be identified as dark areas in the cross section; they are surrounded by a thin white layer of water glass (alkali metal silicates) (Figure 4b).

The macroscopically different bulk structures of granulate and spray-dried silica gels are composed of small, almost spherically shaped particles, which can be seen in an enlarged transmission electron microscopic (TEM) micrograph (Figure 5). The latter

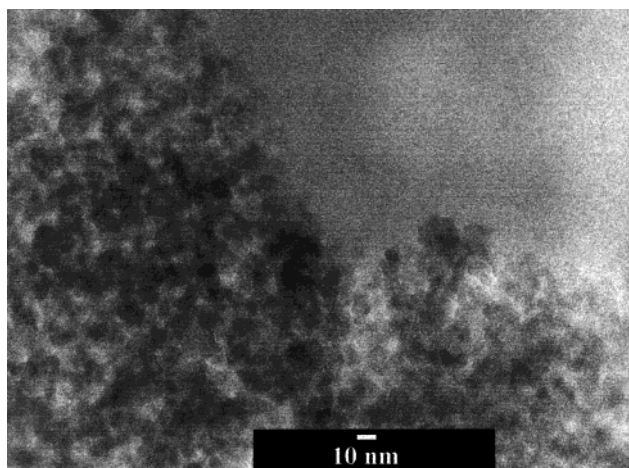


**Figure 5.** HRTEM micrograph of a microtomed thin section of a spray-dried silica gel. The channels between the 10 nm spherical formed primary particles are void pores.

particles have a mean size of approximately 10 nm and form their own pore system, which is recognizable as lighter areas in Figure 5. These primary particles comprise the smallest unit of the silica gels. In his book *The Colloid Chemistry of Silica and Silicates* (1955) Iler<sup>35</sup> proposed a minimum primary particle size of 1 nm. This was later confirmed by Barby,<sup>36</sup> who performed TEM analysis. The primary particles were found to be condensed polysilic acids, which are obtained by reacting water glass and mineral acids. Their size and density are controlled by the unstable transition state of the sol. The high specific surface and the porosity of the particles is caused by the agglomeration of certain primary particles which build up micro- and mesopores. The micropores contribute the main share of the specific surface. Silica gels with a mean average particle size of 2.5 nm, for example, have a specific surface of 1000 m<sup>2</sup>/g.<sup>37</sup>

Regarding the surface of a silica gel at a magnification of 40000:1 (Figure 6), one can see that the 10-

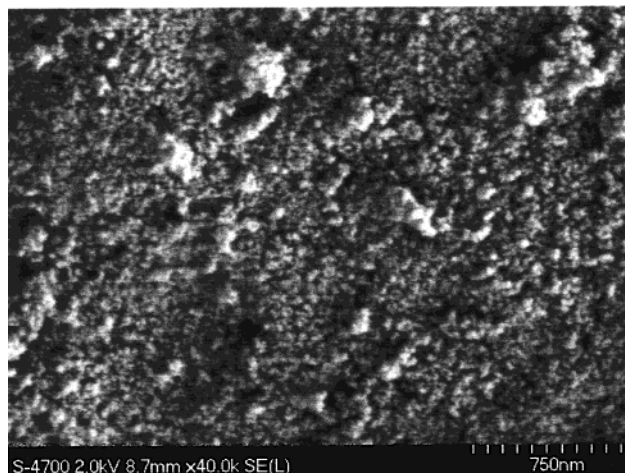


**Figure 6.** Surface microstructure of the spray-dried silica gel. The primary particles are loosely cemented into larger aggregates which, in turn, are packed into even larger clusters of 80–120 nm diameters.

nm-sized primary particles form 80–120 nm-sized silica clusters.

Niegisch<sup>38</sup> has made similar observations for a Davison 952 silica gel used in a Phillips catalysis. He found the smallest units of 10–50 nm, which again form clusters of 200–500 nm.

### III. Supporting Methods and Procedures

The objective of supporting a catalyst is to immobilize and template it in order to get a good polymer morphology in a low-temperature heterogeneous process (i.e., slurry or gas phase), which is usually associated with a loss of activity relative to the homogeneous case. Partial lack of the catalyst components metallocene/MAO on the porous supporting material causes an incomplete fragmentation of the silica gel, which leads to larger amounts of unfragmented silica within the polymer. The resulting polymer is of inferior quality and cannot be used for further processing to, e.g., foils. It is therefore important to choose the right combination of supporting procedure and silica supporting material.

Ribeiro et al. recently described different preparation procedures for MAO-activated metallocene catalysts.<sup>39</sup> According to this comprehensive review, the methods can be divided into three main methods: The first and at the same time oldest method comprises the direct immobilization of the metallocene on a pretreated SiO<sub>2</sub> support.<sup>11,40,41</sup> This method yields only low activities since the metallocenes are decomposed by reaction with the surface OH groups.<sup>6,42</sup> Variations of this method describe the in situ synthesis of metallocene on a support<sup>43,44</sup> and the reaction of metallocene complexes having functional anchors with the support surface, which leads to covalently bonded catalysts on the support.<sup>45,46</sup> Although this procedure has the advantage that the metallocene does not bleed during polymerization and reactor fouling is prevented,<sup>47,48</sup> it is not yet of commercial consequence.

The second method is the reaction of the cocatalyst MAO with the hydroxyl surface of the silica gel, followed by washing, drying, and impregnation with an appropriate zirconocene complex.<sup>7,41,49</sup> Presum-



ably, the absorbed MAO transforms the zirconocene to a "cation like" species. The activity of this material is often inadequate, but it can be augmented with an activator such as  $\text{AlR}_3$  or MAO, which scavenges impurities, alkylates zirconocene complexes, separates ion pairs, etc. The third and best method to produce highly active polymerization catalysts consists of a one-step immobilization of a preactivated MAO/metallocene complex on a porous  $\text{SiO}_2$  support. The activities and the polymer growth can be influenced by choosing distinct concentrations and the viscosity of the organic solvent.<sup>50</sup>

The three supporting methods are related to the chemistry of the catalytic compounds. There is one additional parameter which has an enormous influence on the activity and the impregnation of the catalytically active compounds on the support: reaction engineering. In the following section two different supporting procedures are described, the primarily applied suspension impregnation ( $\text{SiO}_2$ /solved metallocene/MAO compounds) and the gas-phase impregnation (fluidized bed reactor) procedure, which is applied to a smaller extent.

### A. Suspension Impregnation

The distribution degree of the catalytic components on the support is determined by X-ray analysis of bulk cross sections. Our energy-dispersive X-ray (EDX) line scan analysis of a cross section of a suspension-supported particle depicted in Figure 7

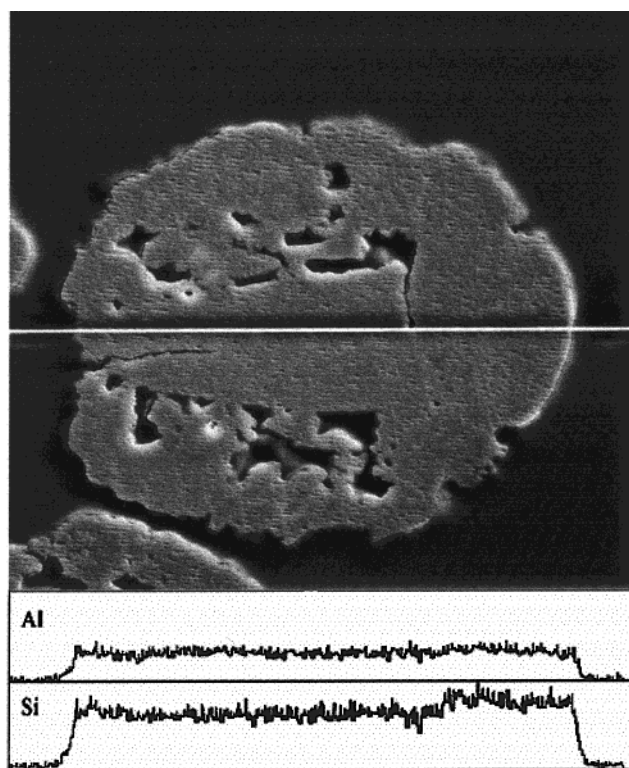


**Figure 7.** EDX line scan analysis of a metallocene/MAO-supported silica gel regarding the silicon and aluminum distribution in the volume.

shows a homogeneous distribution of the cocatalyst MAO. This holds for most of the catalyst particles, although EDX investigations of some suspension-supported particles show that 10–15% have an

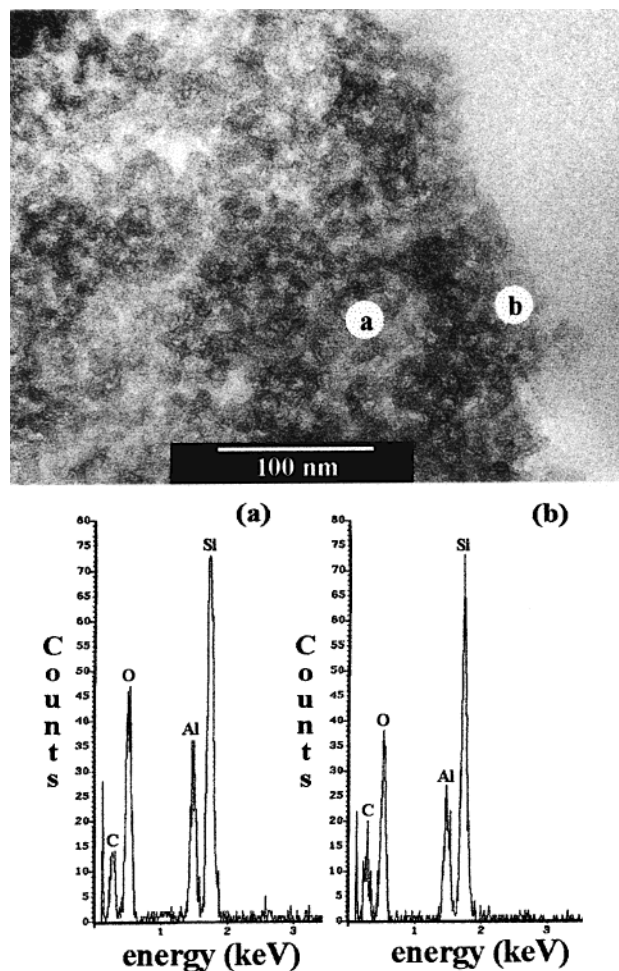


**Figure 8.** (top) HRTEM micrograph of a metallocene/MAO-supported silica gel. The EDX point analysis of the marked areas (a–b) are given in EDX spectra (bottom).

irregular distribution of MAO. The weight percentage of Al on the support usually is 5–10%<sup>41,51</sup> and, therefore, is analytically easily accessible. With a weight percentage of about 0.1–0.3%, the metallocene concentration, however, is distinctly lower than the detection limit and, therefore, cannot be directly determined. It is assumed that both the metallocene component and the MAO are homogeneously immobilized on the support.

Figure 8 shows a combination of a HRTEM micrograph and an EDX point analysis and confirms the homogeneous distribution of MAO in the microstructural region of the support. During the supporting procedure, the metallocene/MAO solution completely penetrates into the micro- and mesopores of the silica gel, without formation of a concentration gradient. BET measurements were carried out to investigate changes in the pore size distribution of the supported silica gels. These measurements revealed that while reacting with the silica gel the MAO component does not simply cover the outer surface of the particle and fill up the inside of the pores, but builds up a pore structure itself. The portion of pores with medium and larger pore radii (10–40 nm) are filled up in the course of the immobilization. The loss of specific surface is compensated by newly formed pores with smaller radii (1–5 nm).<sup>52</sup>

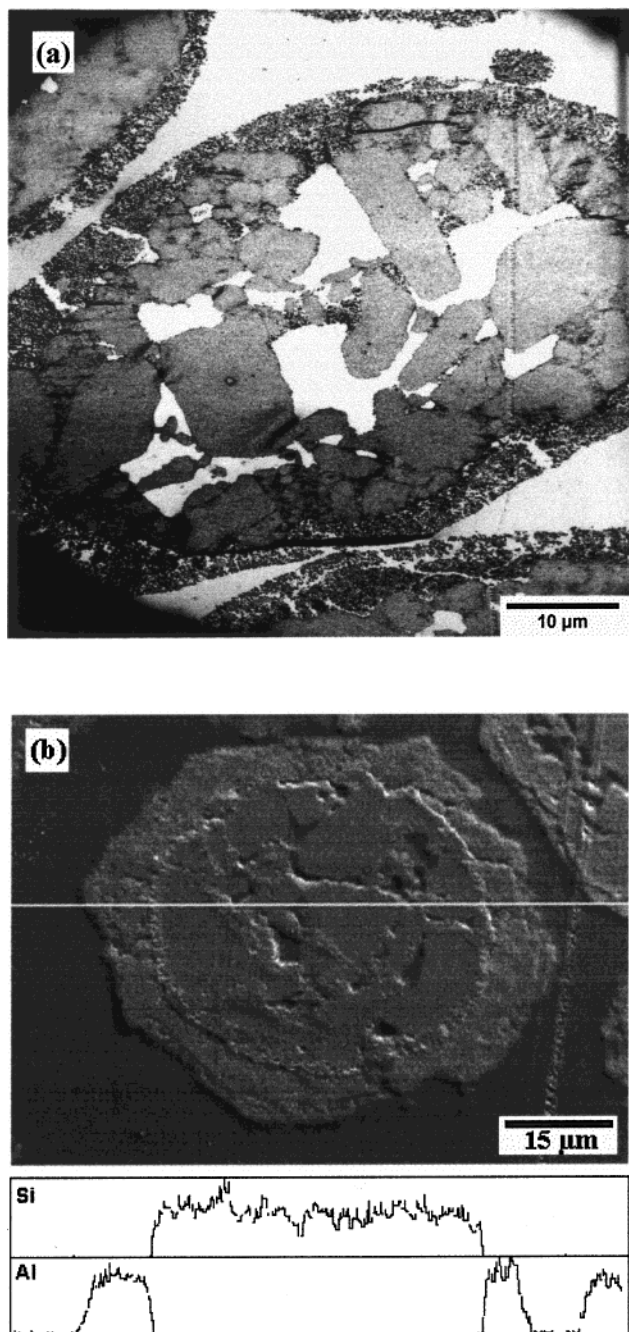


**Figure 9.** (a) TEM micrograph of a supported metallocene/MAO catalyst particle prepared by gas-phase impregnation with TMA/H<sub>2</sub>O. (b) EDX line scan analysis of the metallocene/MAO-supported silica gel regarding the silicon and aluminum distribution in the volume. Under this condition, the active sites are formed on the outer surface of the particle. The mean particle size shifted from 50  $\mu\text{m}$  for the silica support to 70  $\mu\text{m}$  for the catalyst.

## B. Gas-Phase Impregnation

As an alternative to the suspension process, Witco GmbH developed (1995) a technique which immobilizes the active compounds on a spray-dried silica support by utilizing a fluidized bed reactor. They claimed to produce supported metallocene catalysts with a controllable distribution of active centers achieved by using the three different supporting methods.<sup>53,54</sup> Controlling the addition of trimethylaluminum and water in the different reactor

zones it is possible to produce catalyst systems with a homogeneous and inhomogeneous distribution of MAO on the porous support. The metallocene component is added to the support after the formation of MAO. Figure 9 presents a catalytic system in which MAO was not formed in the pore system by diffusing TMA but instead was already obtained in the reaction zone due to the controlled dosage of water and TMA.<sup>55</sup>

The large MAO drops cover the outer surface of the particle as a thin layer, thereby sealing the outer pores and preventing further diffusion into the inner cavities. The EDX analysis presented in Figure 9b confirms the completely MAO-free particle interior.

## IV. Polymerization Kinetics

The kinetics of a propene polymerization which is promoted by SiO<sub>2</sub>-supported metallocene catalysts depends on various factors: (1) On the applied reaction engineering (gas-phase,<sup>56</sup> bulk,<sup>57</sup> and slurry polymerization);<sup>50</sup> (2) On the degree of catalyst/cocatalyst distribution on the support; and (3) On the chosen reaction conditions and parameters (Figure 10).<sup>58</sup>

A high polymerization temperature and concentration of active species on the support lead to an increase in polymerization activity, as well as a high monomer concentration in the reacting solution. A detailed kinetic investigation of the polypropene growth using metallocenes prepared by suspension impregnation is facilitated by choosing especially mild reaction conditions (low temperature, low catalyst concentration, low monomer concentration). In doing so it is possible to resolve the individual phases of polymerization and polymer growth from the start of the reaction. The polymerization rate/time plot (Figure 10a,  $T_{\text{polym}} = 40\text{ }^{\circ}\text{C}$ ) shows a course which is characteristic of these systems under the chosen conditions. The reaction starts with a short increase in activity, the “prepolymerization period”, followed by a drop of the reaction velocity to almost zero. The low level is kept for some minutes, in the case of supported metallocene catalysts the length of this “induction period” can vary distinctively. After the induction period the activity rises again (“polymer growth”) until a plateau of maximum activity is reached (“particle expansion”).

The individual kinetic stages of the propene polymerization, which were elucidated by detailed electron microscopic studies, can be interpreted as follows. During the prepolymerization stage the polymer forms a regular thin layer around the particle, which partially continues to grow into the marginal areas of the micro- and mesoporous silica gel. The layer of highly crystalline polypropene (up to 75%) serves as a diffusion barrier for following propene and induces the induction period of very low activity. As the polymerization time increases, the polymer growth from the outside to the inside continues accompanied by a slowly beginning fragmen-



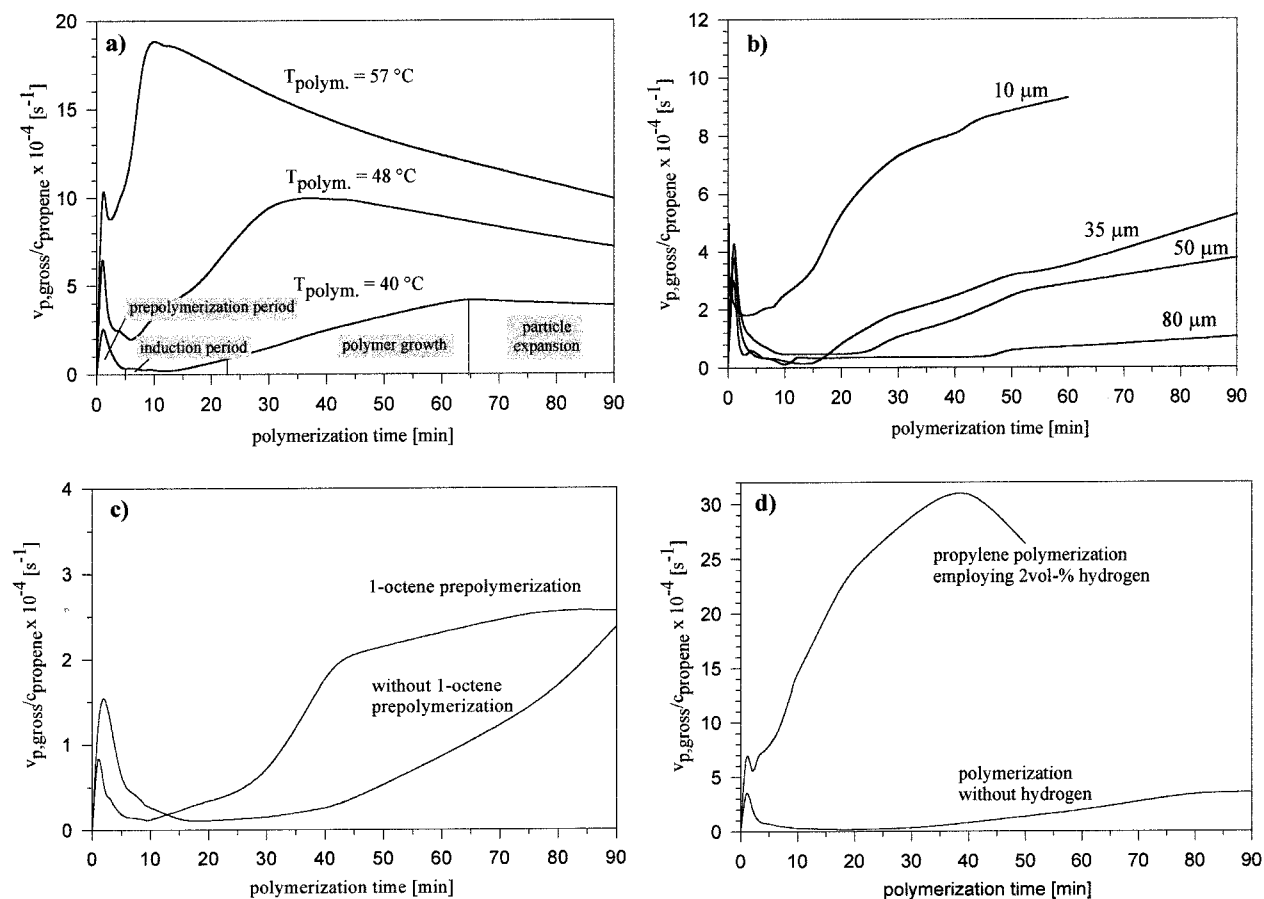


**Figure 10.** Propene polymerization profiles of a silica-supported metallocene/MAO catalyst prepared by suspension impregnation: (a) depending on polymerization time and polymerization temperature and (b) depending on particle size and polymerization time. (c) Comparison of the activity profiles between an 1-octene prepolymerized catalyst and an untreated system. (d) Comparison of the activity profiles between a catalyst system employing 2 vol % hydrogen and the not activated system.

tation of the support. This fragmentation produces new active centers, and the reaction proceeds until the highest possible activity is reached and the whole support is fragmented in the polymer. The crystallinity of the polypropene decreases also with increasing polymerization time (50% crystallinity at 30 min polymerization time, 30% crystallinity at 90 min) and the diffusion barrier for the propene is reduced.

Increasing the polymerization temperature from 40 to 48 or 57  $^\circ\text{C}$ , respectively, leads to a rise of the total activity of the catalyst system and a shift of the maximum activity to shorter reaction times (Figure 10a). At the same time the induction period shortens, nevertheless retaining the prepolymerization maximum. Therefore, an increase in temperature yields a more active catalysts system for propene polymerization. This gain in activity leads to an increase of the velocity with which the individual stages of polymerization are passed.

If the catalyst particle diameter is varied (Figure 10b), it is also possible to influence the kinetics and total activity of the system. The larger the particle diameter is, the longer the induction period takes and the slower the reaction velocity increases. This is partially due to the smaller outer surface of a larger particle compared to a smaller particle with the same amount of catalyst. Another reason is the particle

fragmentation, which starts earlier for small particles, since less volume is connected with less diffusion limitation of the polymer layer.

Apart from the increase in temperature or the use of smaller catalyst particles, there are additional possibilities to shorten the induction period and to improve the polymerization kinetics. The amorphous poly(1-octene) layer on the particle which is generated by a prepolymerization of 1-octene causes a less significant diffusion limitation for the monomer gas compared to the one induced by a highly crystalline polypropene layer (Figure 10c). As another alternative, the active centers are chemically activated by the addition of gaseous hydrogen during propene polymerization.<sup>59</sup> This interesting phenomenon was first observed for a  $\text{MgCl}_2$ -supported catalyst<sup>60</sup> and confirmed for the phthalate/alkoxysilane systems.<sup>61–63</sup> The addition of hydrogen to the reactor leads to a drastic increase in activity (Figure 10d). The hydrogen which diffuses easily through the polymer layer activates sterically hindered sites for regioselective insertions of propene.<sup>64–67</sup>

## V. Polymer Morphology

The morphology of the polymer particle depends strongly on the form of the employed  $\text{SiO}_2$  support.



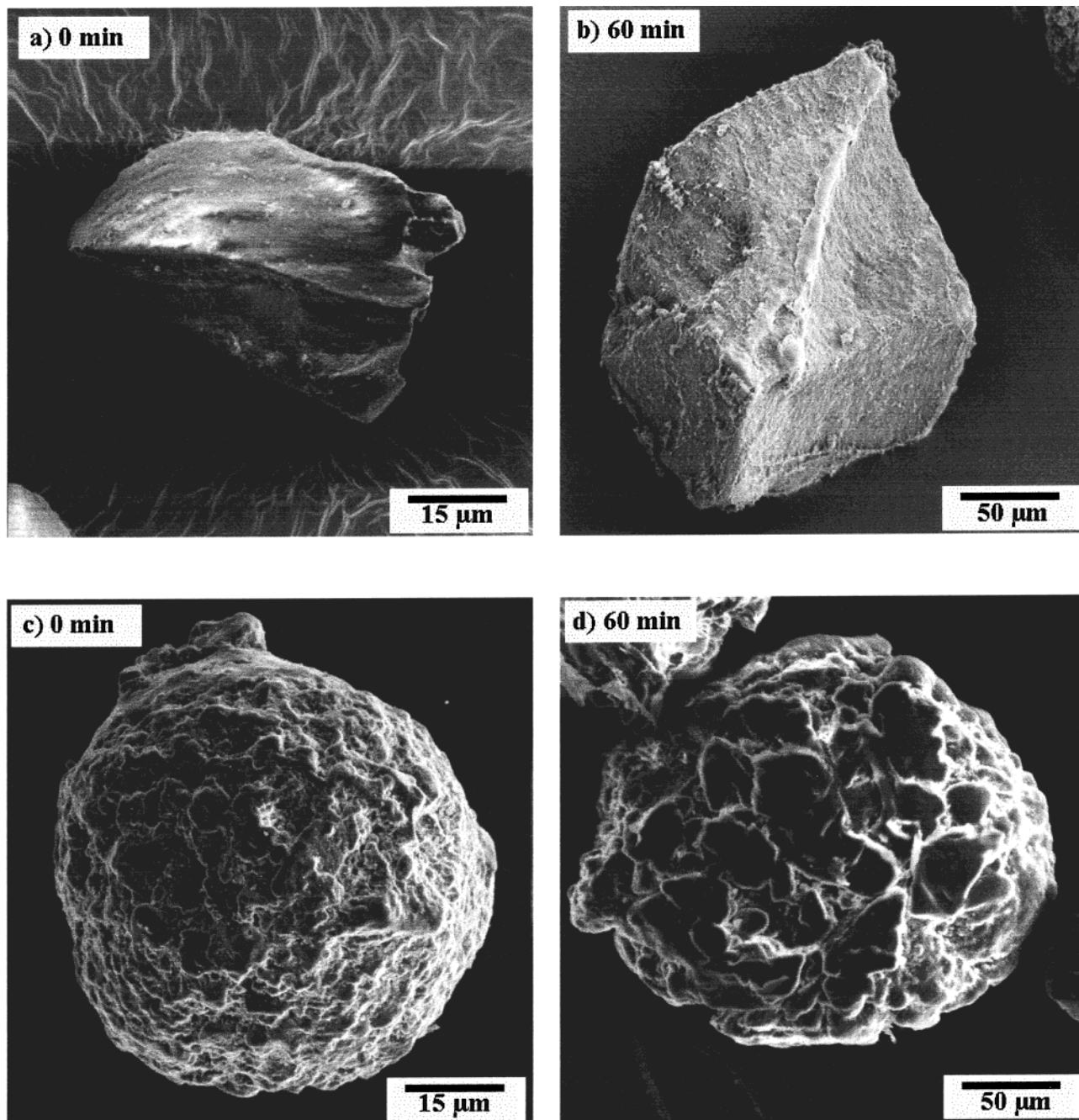


**Figure 11.** SEM micrographs of the metalocene/MAO-supported granular (a) and spray-dried silica gels (c) and of their polymer products (b,d). The polymer particles show the identical morphology of the supporting materials with the difference that the particle size has increased by the factor of 3.

If edged, ungeometric  $\text{SiO}_2$  granulate particles are employed (Figure 11a); the resulting polymer is an exact replica of the support (Figure 11b). If, however, spray-dried spherical particles are used (Figure 11c), the obtained polymer particles are spherical as well (Figure 11d).

Detailed transmission and scanning electron microscopic studies of shortly polymerized  $\text{SiO}_2$ -supported metallocene catalysts facilitated the time-resolved representation of the morphology of the various polymerization stages from the start of the reaction until the maximum activity was reached.

The SEM micrographs of a catalyst system polym-

erized for 5 min (Figure 12a,b) show that the polymerization starts at the most easily accessible centers on the particle surface and that a thin, net-like layer of polypropene is formed. With increasing polymerization time (Figure 12c,d) a compact polymer layer is built; the particle diameter, however, rises only insignificantly during the induction period due to the low activity. Only after distinctly leaving the induction period does the morphology conserving particle growth continue along with the polymer growth.

It was intended to observe the initial polymer growth directly below the forming polymer shell. Therefore, the active centers on the particle sur-

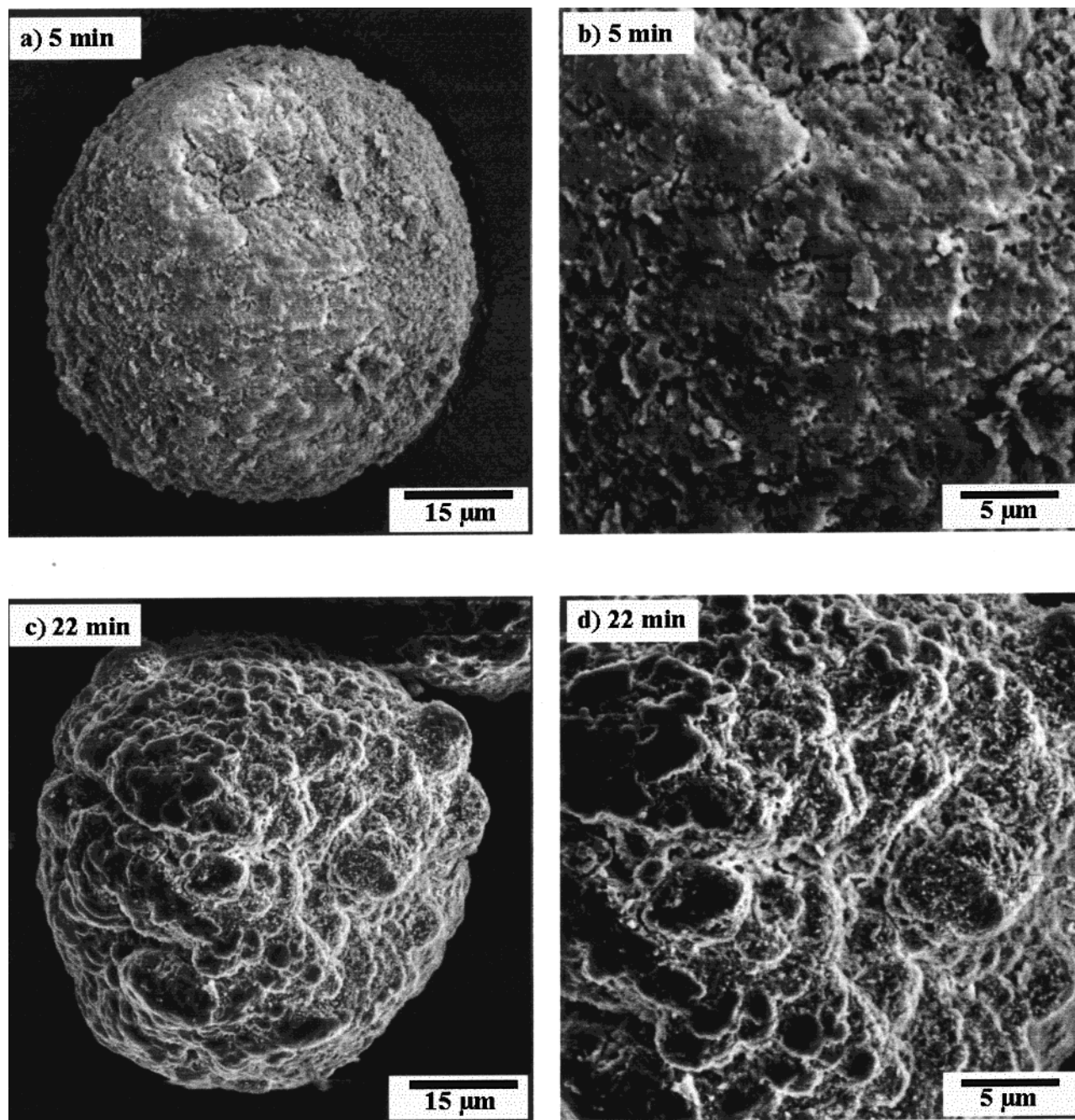


**Figure 12.** SEM micrographs of a metallocene/MAO-supported spray-dried silica gel after a polymerization time of 5 and 22 min. The enlarged polymer morphology is shown in a magnification on the right side.

face were specifically deactivated, and a catalyst prepared in such way was used for a propene polymerization. The SEM micrographs presented in Figure 13 show the surface of a particle polymerized for 5 min. A heterogeneous polymer growth takes place producing polymer strings of defined structure. These strings clearly derive from the sub-surface of the particle. They break up the porous silica gel layer and thereby enable further fragmentation of the support. As a consequence of the turbulent mixing of the catalyst particle in the reactor, the position of the polymer strings on the surface is disordered.

These SEM investigations show for the first time how the polymer, which is formed in the

pores of the silica gel, is able to use its hydraulic forces and mechanically break up the structure of the support, thereby setting free new active centers.

The morphology control of the polymer is not only caused by the support, but also by its fragmentation and the resulting distribution of catalyst and cocatalyst on the support during polymerization. This was clarified by analyzing a catalytic system, the active centers of which are exclusively on the surface and the volume of which is completely free of catalyst.<sup>55</sup> For this reason, the polymerization can only take place on the outside and even after long polymerization times the support remains unfragmented and covered by the polymer (Figure



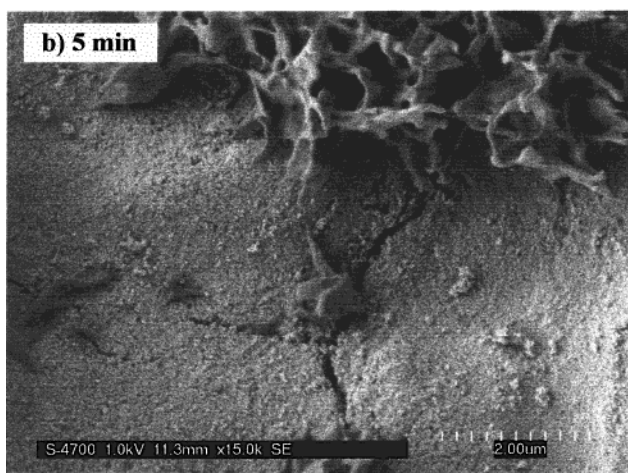
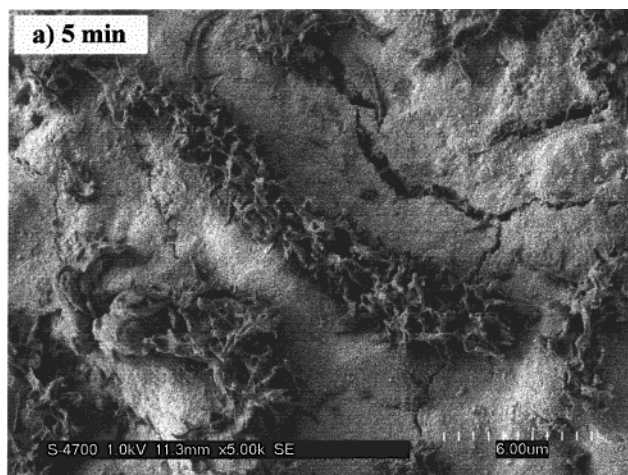


**Figure 13.** Enlarged SEM micrographs of a deactivated catalyst surface after a polymerization time of 5 min. The polymer starts growing from an internal layer by breaking up the outer  $\text{SiO}_2$  surface.

14). The obtained polymer morphologies are not uniform and depend on the form of the employed silica gel.

## VI. Fragmentation Process

The morphological studies of catalyst systems polymerized for different times revealed that the particle growth starts only after distinctly exceeding the induction period and proceeds continually as the polymerization activity increases. The onset of fragmentation of the support is a prerequisite for the particle growth and the simultaneous conservation of morphology.

To achieve fragmentation of the porous support, the hydraulic forces produced by polymerization within the micro- and mesopores have to be sufficiently high. During the induction period a regular polymer layer forms around the particle (Figure 15a), accompanied by the splitting of small  $\text{SiO}_2$  fragments from the surface of the support (Figure 15b). At the same time, monomer diffuses into the marginal regions of the silica gel which are then filled with polymer (Figure 16a).

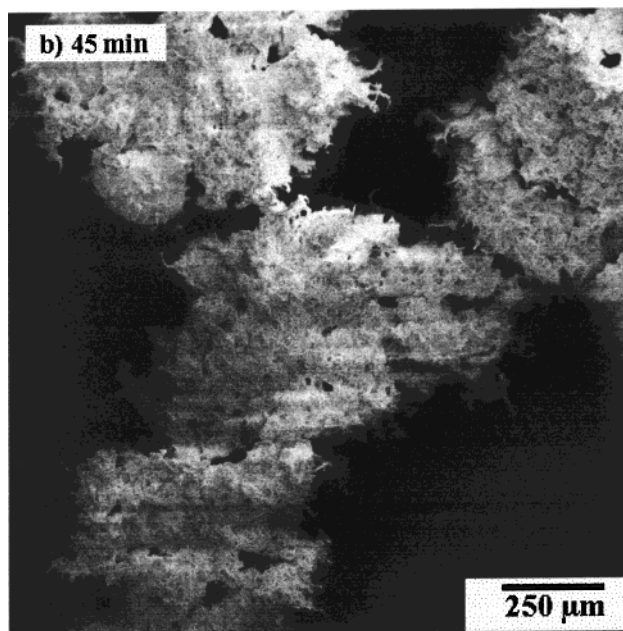
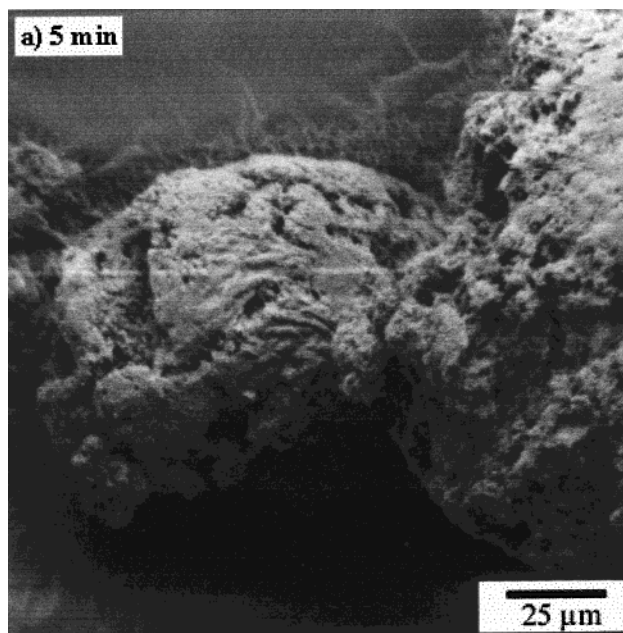


**Figure 14.** SEM micrographs of a supported metallocene/MAO catalyst particle prepared by gas-phase impregnation after a polymerization time of 5 and 45 min. The active sites are located exclusively on the outer surface of the supporting material, and the absence of the particle fragmentation during the polymerization leads to an uncontrolled polymer morphology.

The produced polymer layer, which consists of approximately 70% crystalline polypropene, strongly impedes the diffusion of monomer and is responsible for the decrease of the total activity to a low level. At this polymerization stage the hydraulic forces in the outer regions of the particle are not sufficient to induce fragmentation of the support (Figure 16b).

With increasing polymerization time, the polymer growth slowly continues from the outside to the inside of the pore system of the  $\text{SiO}_2$  support. The



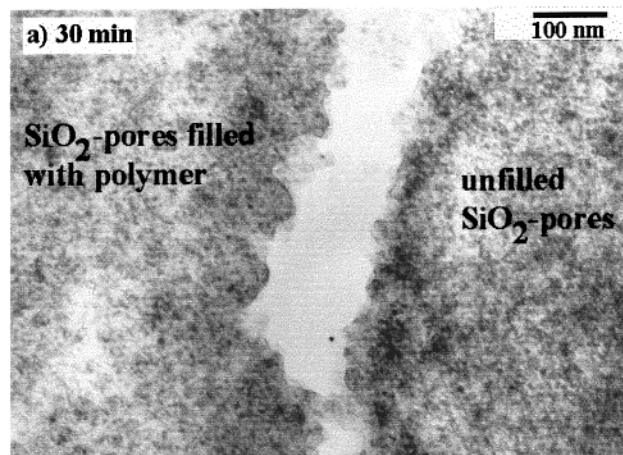
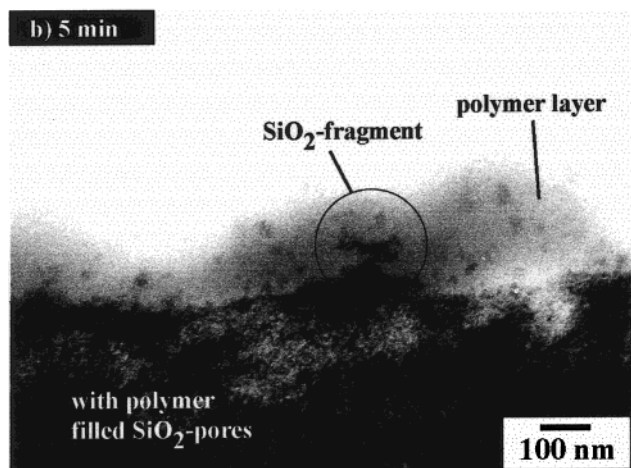
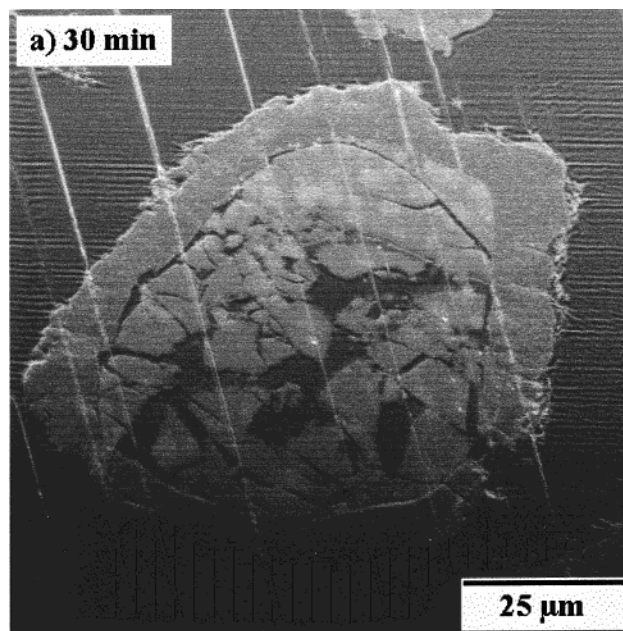
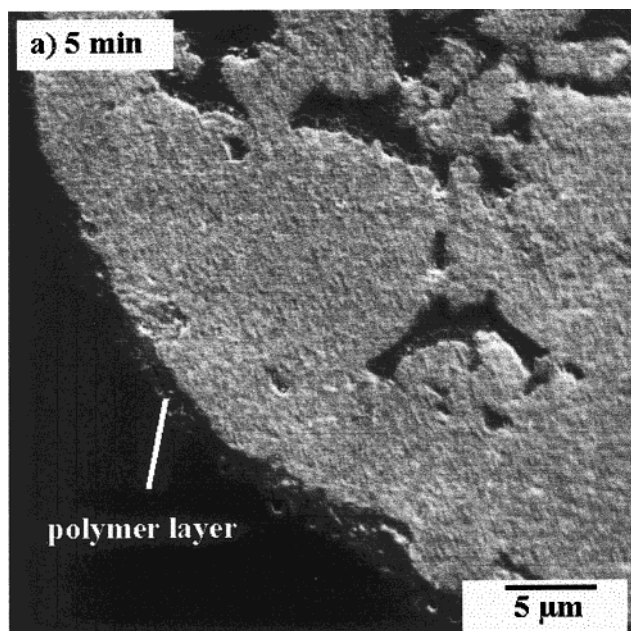


**Figure 15.** (a) SEM micrographs of a catalyst particle after a polymerization time of 5 min. The bulk structure reveals the starting points of the propene polymerization at the outer and inner surface of the silica gel. (b) This polymer layer includes small SiO<sub>2</sub> fragments which were separated from the support during the polymerization process (TEM).

**Figure 16.** (a) SEM micrographs of a catalyst particle after a polymerization time of 30 min. The polymer layer grows with increasing polymerization time from the outside into the inner part of the particle. (b) The HRTEM micrographs indicate the filling of the micro- and mesopores of the silica gel without fragmentation of the supporting material.

slowly beginning particle fragmentation sets free new active centers and causes an increase in polymerization activity. As the maximum activity is reached, the SiO<sub>2</sub> support is completely fragmented and homogeneously distributed in the polymer matrix (Figure 17a). The size of the SiO<sub>2</sub> fragments, which consist of agglomerates of small, 10-nm-sized spherical primary particles (Figure 17b), vary from 30 to 200 nm. These agglomerates comprise the smallest unit of the support, particle sizes cannot—even in the course of longer polymerization times—fall below the size of this unit. The size of the fragments seems to be governed by the preparation procedure of the silica gels, which consist of 50–100 nm clusters, which themselves are based on 10 nm primary particles.

## VII. Conclusions

Electron microscopic studies of the polymer morphology and the fragmentation of the support lead to the clarification of the chronological course of a propene polymerization on SiO<sub>2</sub>-supported metallocene catalysts (Figure 18). According to these findings, the polypropene growth on SiO<sub>2</sub>-supported metallocene catalysts can be described by a “particle growth model” which was developed (1995) in our group<sup>52</sup> and is now refined.<sup>68</sup> This model was successfully applied for a mathematical simulation of the polymerization process. It was also successfully transferred to the mathematical simulation of the polymerization kinetics affiliated with differently sized grain diameters.<sup>68</sup> Part of the polymerizations were carried out in liquid monomer to confirm that at least



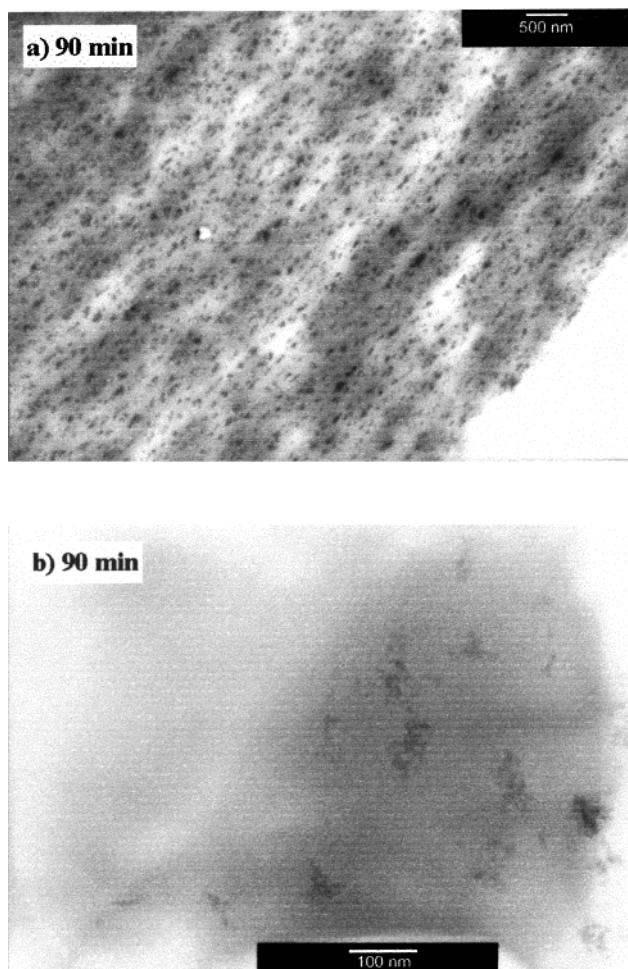


**Figure 17.** Microtomed thin sections (HRTEM) of a catalyst particle after a polymerization time of 90 min. The silica gel support is homogeneously distributed in the polymer matrix (a). The magnified micrograph (b) reveals the 50–100 nm SiO<sub>2</sub> fragments as an agglomeration of primary particles.

at low temperatures the model also holds for the industrially relevant mass polymerizations.<sup>57</sup> Prepolymerization experiments with 1-octene showed that the kinetics of both slurry and mass processes can

be influenced in a way that the induction period is significantly shortened and the reaction is accelerated. The decrease of crystallinity of the initially formed polymer shell as the shell is changed from polypropene to poly(1-octene) plays a key role in this process. Furthermore, it is possible to eliminate the induction period by adding small amounts of gaseous hydrogen to the propene polymerization under retention of the polymer morphology.<sup>59</sup>

Later the growth model developed for a neodymium catalyst system was applied for the butadiene polymerization in gas phase. The ideas concerning the initial polymerization stages are in agreement with a “core–shell model”.<sup>69,70</sup> The subsequent polymerization stages correspond to the “polymeric flow model”.<sup>71,72</sup>

Due to these kinetic and electron microscopic investigations of SiO<sub>2</sub>-supported metallocene catalysts for propene polymerization, it was possible for the first time to gain insights into the operation of the support and the different polymer growth processes. Further attempts will be focused on the development of model supports for metallocene catalysts, with which the polymer growth can be studied on well-defined reproducible two-dimensional support surfaces. Magni and Somarjai<sup>73,74</sup> were the first to report on a successful model Ziegler catalyst which polymerized ethylene and propene at good yields. Two years later, a planar surface model for a Phillips catalyst was introduced by a Dutch group headed by Thüne and Niemantsverdriet.<sup>75,76</sup>

To determine the degree of distribution of a metallocene catalyst despite its low concentration on the support, we investigated a radioactive label method that allows us to locate the catalyst with an good spatial resolution by means of electron microscopy.

Additional approaches concern the determination of single diffusion coefficients at various polymerization stages and while using polymeric support for the covalent fixing of the metallocene components.

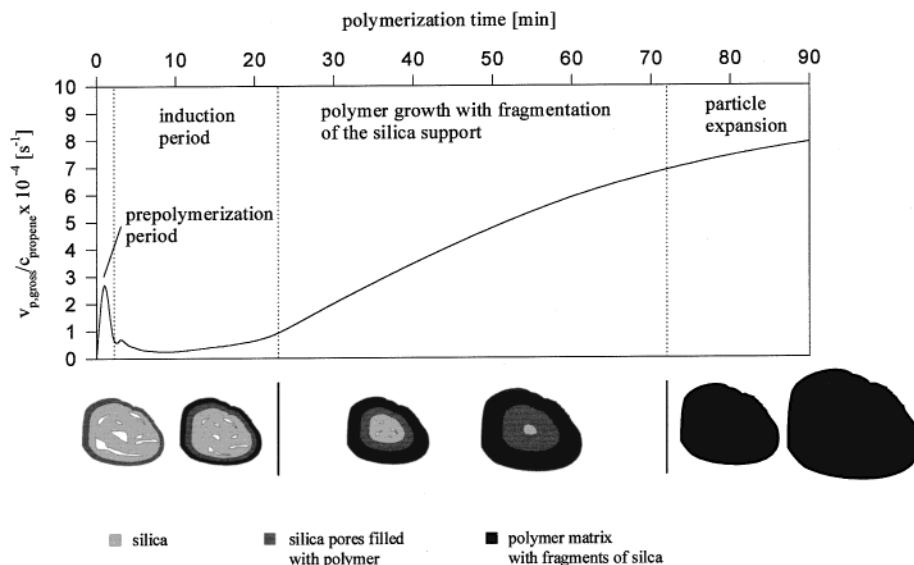


**Figure 18.** Schematic particle growth model for the propene polymerization of a silica-supported metallocene/MAO catalyst.

### VIII. Acknowledgment

We gratefully acknowledge Targor GmbH and BASF AG for the seminal cooperation.

### IX. References

- (1) Kuhlke, W. C. *Hydrocarbon Process.* **1997**, I-3.
- (2) *Nachr. Chem. Tech. Lab.* **1995**, 43, 1208.
- (3) *Eur. Chem. News* **1997**, 1637.
- (4) Karol, F. J. *Macromol. Symp.* **1995**, 89, 563.
- (5) Hogan, J. P.; Norwood, D. D.; Ayres, C. A. *J. Appl. Polym. Sci., Appl. Polym. Symp.* **1981**, 36, 49.
- (6) Collins, S.; Kelly, W. M.; Holden, D. A. *Macromolecules* **1992**, 25, 1780.
- (7) Chien, J. C. W.; He, D. *J. Polym. Sci., Part A: Polym. Chem.* **1991**, 29, 1603.
- (8) Janiak, C.; Rieger, B. *Angew. Makromol. Chem.* **1994**, 215, 47.
- (9) Chien, J. C. W.; Wang, B.-P. *J. Polym. Sci., Part A: Polym. Chem.* **1988**, 26, 3089.
- (10) Chien, J. C. W.; Wang, B.-P. *J. Polym. Sci., Part A: Polym. Chem.* **1990**, 28, 15.
- (11) Kaminaka, M.; Soga, K. *Macromol. Rapid Commun.* **1991**, 12, 367.
- (12) Arribas, G.; Conti, G.; Altomare, A.; Ciardelli, F. *Proc. Int. Symp. Synth., Struct. Ind. Aspects Stereospec. Polym. STEPOL* **1994**, 94, 210.
- (13) Ismayel, A.; Sanchez, G.; Arribas, G.; Ciardelli, F. *Mater. Eng.* **1993**, 4, 267.
- (14) Woo, S.; Ko, Y.; Han, T. *Macromol. Rapid Commun.* **1995**, 16, 489.
- (15) Janiak, C.; Rieger, B.; Völkel, R.; Braun, H. G. *J. Polym. Sci., Part A: Polym. Chem.* **1993**, 31, 2959.
- (16) Lee, D. H.; Yoon, K. B. *Macromol. Rapid Commun.* **1994**, 15, 841.
- (17) Soga, K.; Arai, T.; Hoang, B. T.; Uozumi, T. *Macromol. Rapid Commun.* **1995**, 16, 905.
- (18) Nishida, H.; Uozumi, T.; Arai, T.; Soga, K. *Macromol. Rapid Commun.* **1995**, 16, 821.
- (19) Stork, M.; Koch, M.; Klapper, M.; Müllen, K.; Gregorius, H.; Rief, U. *Macromol. Rapid Commun.* **1999**, 20, 210.
- (20) Pfeifer, B.; Milius, W.; Alt, H. G. *J. Organomet. Chem.* **1998**, 553, 205.
- (21) Alt, H. G.; Jung, M. *J. Organomet. Chem.* **1998**, 562, 229.
- (22) *J. Organomet. Chem.* **1998**, 562, 153.
- (23) Unger, K. K. *Ber. Bunsen-Ges. Phys. Chem.* **1975**, 79, 149.
- (24) Unger, K. K. *Poros silica. J. Chromatogr. Libr.* **1979**, 16, xxx.
- (25) Flemmert, G. L. *Proc.-Fert. Soc.* **1977**, 163.
- (26) IUPAC, Manual of Symbols and Terminology, Appendix 2, Part I, Colloid and Surface Chemistry, *Pure Appl. Chem.* **1972**, 31, 578.
- (27) Chien, J. C. W. *J. Am. Chem. Soc.* **1971**, 93, 4675.
- (28) Chien, J. C. W. *J. Catal.* **1971**, 73, 71.
- (29) Kiselev, A. V.; Lygin, V. I. *Infrared Spectra of Surface Compounds*; Wiley-Interscience: New York, 1975.
- (30) Hair, M. L. *Infrared Spectroscopy in Surface Chemistry*; Marcel Dekker: New York, 1967.
- (31) Chien, J. C. W. *Top. Catal.* **1999**, 7, 23.
- (32) Wagner, A.; Schmidt, F.; Bauer, D.; Kerner, D. (Degussa), *EP-A 0341 383*, 1989.
- (33) Kirkland, J. J. U.S. Patent 3,782,075, 1974.
- (34) McQueston, H. J.; Iler, R. K. U.S. Patent 3855172, 1974.
- (35) Iler, R. K. *Colloid Chemistry of Silica and Silicates*; Iler, R. K., Ed.; Cornell University Press: Ithaca, NY, 1955.
- (36) Barby, D. *Characterization of powder surfaces*; Sing, K. S. W., Parfitt, G. D., Ed.; Academic Press: London, 1976.
- (37) Welsh, W. A. *Ullmann's Encyclopedia of Industrial Chemistry*; VCH Verlagsgesellschaft, 1993; Vol. A23, p 629.
- (38) Niegisch, W. D.; Crisafulli, S. T.; Nagel, T. S.; Wagner, B. E. *Macromolecules* **1992**, 25, 3910.
- (39) Ribeiro, M. R.; Deffieux, A.; Portela, M. F. *Ind. Eng. Chem. Res.* **1997**, 36, 1224.
- (40) Soga, K.; Kaminaka, M. *Makromol. Chem.* **1993**, 194, 1745.
- (41) Kaminsky, W.; Renner, F. *Macromol. Rapid Commun.* **1993**, 14, 239.
- (42) Sacchi, M. C.; Zucchi, D.; Tritto, I.; Locatelli, P.; Dall' Occo, T. *Macromol. Rapid Commun.* **1995**, 16, 581.
- (43) Soga, K.; Kim, H. J.; Shiono, T. *Macromol. Rapid Commun.* **1994**, 15, 139.
- (44) Jin, J.; Uozumi, T.; Soga, K. *Macromol. Rapid Commun.* **1995**, 16, 317.
- (45) Lee, D.-H.; Yoon, K.-B. *Macromol. Rapid Commun.* **1997**, 18, 427.
- (46) Suzuki, N.; Asami, H.; Nakamura, T.; Huhn, T.; Fukuoka, A.; Ichikawa, M.; Saburi, M.; Wakatski, Y. *Chem. Lett.* **1999**, 341.
- (47) Bonds, W. D.; Brubaker Jr., C. H.; Chandrasekaran, E. S.; Gibbons, C.; Grubbs, R. H.; Kroll L. C. *J. Am. Chem. Soc.* **1975**, 97, 2128.
- (48) Petrucci, M. G. L.; Kakkar, A. K. *J. Chem. Soc., Chem. Commun.* **1995**, 1577.
- (49) Chen, Y.-X.; Rausch, M. D.; Chien, J. C. W. *J. Polym. Sci., Part A: Polym. Chem.* **1995**, 33, 2093.
- (50) Steinmetz, B.; Tesche, B.; Przybyla, C.; Zechlin, J.; Fink, G. *Acta Polym.* **1997**, 48, 392.
- (51) Soga, K.; Kaminaka, M. *Macromol. Rapid Commun.* **1992**, 13, 221.
- (52) Bonini, F.; Fraaije, V.; Fink, G. *J. Polym. Sci., Part A: Polym. Chem.* **1995**, 33, 2393.
- (53) EP Patent (Witco GmbH) 0,763,546, 1995.
- (54) EP Patent (Witco GmbH) 0763 545, 1995.
- (55) Goretzki, R.; Fink, G.; Tesche, B.; Steinmetz, B.; Rieger, R.; Uzick, W. *J. Polym. Sci., Part A: Polym. Chem.* **1999**, 37, 677.
- (56) Roos, P. R.; Meier, G. B.; Samson, J. J.; Weickert, G.; Westerterp, K. R. *Macromol. Rapid Commun.* **1997**, 18, 319.
- (57) Zechlin, J.; Hauschild, K.; Fink, G. *Macromol. Chem. Phys.*, in press.
- (58) Przybyla, C.; Zechlin, J.; Steinmetz, B.; Tesche, B.; Fink, G. *Metalorganic catalysts for synthesis and polymerization*; Kaminsky W., Ed.; Springer-Verlag: Berlin 1999; p 321
- (59) Zechlin, J.; Steinmetz, B.; Tesche, B.; Fink, G. *Macromol. Chem. Phys.*, in press.
- (60) Guastalla, G.; Giannini, U. *Macromol. Chem., Rapid Commun.* **1983**, 4, 519.
- (61) Spitz, R.; Masson, P.; Bobichon, C.; Guyot, A. *Makromol. Chem.* **1989**, 190, 717.
- (62) Parsons, I. W.; Al-Turki, T. M., *Polym. Commun.* **1989**, 30, 72.
- (63) Kioka, M.; Kashiwa, N. *J. Macromol. Sci., Chem.* **1991**, A28, 865.
- (64) Kojoh, S.; Kioka, M.; Kashiwa, N.; Itoh, M.; Mizuno, A. *Polymer* **1995**, 36, 5015.
- (65) Mori, H.; Tashino, K.; Terano, M. *Macromol. Rapid Commun.* **1995**, 196, 651.
- (66) Chadwick, J. C.; van Kessel, G. M. M.; Sudjmeier, O. *Macromol. Chem. Phys.* **1995**, 196, 1431.
- (67) Carvill, A.; Tritto, I.; Locatelli, P.; Sacchi, M. C. *Macromolecules* **1997**, 30, 7056.
- (68) Przybyla, C.; Zechlin, J.; Weimann, B.; Fink, G. *Metalorganic Catalysts for Synthesis and Polymerization*; Kaminsky W., Ed.; Springer-Verlag: Berlin 1999; p 333.
- (69) Schmeal, W.-R.; Street, J. R. *AIChE J.* **1971**, 17, 1188.
- (70) Nagel, E. J.; Kirillov, V. A.; Ray, W. H. *Ind. Eng. Chem. Prod. Res. Dev.* **1980**, 19, 372.
- (71) Soares, J. B. S.; Hamielec, A. E. *Polym. React. Eng.* **1995**, 3, 261.
- (72) Soares, J. B. S.; Hamielec, A. E. *Polym. React. Eng.* **1996**, 4, 153.
- (73) Magni, E.; Somorjai, G. A. *Catal. Lett.* **1995**, 35, 205.
- (74) Koranyi, T. I.; Magni, E.; Somorjai, G. A. *Top. Catal.* **1999**, 7, 179.
- (75) Thüne, P. C.; Verhagen, C. P. J.; van den Boer, M. C. G.; Niemantsverdriet, J. W. *J. Phys. Chem. B* **1997**, 101, 8559.
- (76) Thüne, P. C.; Loos, J.; Lemstra, P. J.; Niemantsverdriet, J. W. *J. Catal.* **1999**, 183, 1.

CR9804689